The influence of thermal treatment on properties of kaolin

Elizabeth Erasmus

Department of Chemistry, University of the Free State, Bloemfontein, Republic of South Africa

Abstract

The kinetics of dehydroxylation of South African kaolin revealed that both the inner and the surface hydroxyl groups disappear according to first order kinetics, however, the surface group disappeared faster than the inner groups, showing that diffusion control kinetics is also important. The temperature dependent transformations of the kaolin was measured by means of fractional conversion of the ratios between AlO_6:AlO_4 and Si-O-Al:Si-O-Si, which showed k_{obs} values 0.0168 s^{-1} and 0.0089 s^{-1} for the transformation to the spinel phase and values of 0.0165 s^{-1} and 0.0156 s^{-1} for the transformation to mullite respectively. The pozzolanic activities of the kaolin calcined at different temperatures showed a maximum pozzolanic activity when the kaolin is calcined at 650°C and the pozzolanic activity for mullite is even less than for the uncalcined kaolin. XPS revealed that the atomic ratio between Si and Al did not change from kaolin to metakaolin (Si:Al = ca. 1.2) however the mullite showed a atomic ratio of Si:Al = 1.52, implying that some deallumination occurred during calcination at high temperatures.

Keywords: dehydroxylation, kaolin, metakaolin, infra-red, pozzolanic activity, mullite.

Available online at the Journal website: http://www.ache.org.rs/HI/

SCIENTIFIC PAPER

UDC 66.094.32.091.8:553.612(6)

Hem. Ind. **70** (5) 595–601 (2016)

doi: 10.2298/HEMIND150720066E

Kaolin is a naturally occurring clay mineral with kaolinite being the main component having a chemical composition of $Al_2Si_2O_5(OH)_4$. It has a layered silicate structure, where oxygen atoms link an octahedral sheet of alumina with a tetrahedral sheet of silica.[1] When kaolinite is calcined at elevated temperatures, dehydroxylation occurs which collapses the crystal structure to produce amorphous metakaolinite ($Al_2Si_2O_7$) [2], according the following proposed reaction scheme:[3]

$$Al_2Si_2O_5(OH)_4 \rightarrow Al_2Si_2O_7 + 2H_2O\uparrow$$

The thermal transformation of metakaolinite above 1000 °C first produces either a Al–Si spinel phase or a aluminasilicate phase [2] which transforms into mullite [4] and above 1150 °C cristobalite (*c*-SiO_2) is formed.

The thermal transformation of kaolin has been the subject of numerous studies, which reported on how the different heating conditions influence the dehydroxylaton process.[4–8].

At temperature below 400 °C, a reversible dehydroxylation process takes place, upon cooling the hydroxyl peaks reappear in the infrared spectra [9]. Above temperatures of 400 °C irreversible loss of hydroxyl groups occur. The temperature at which the highest rate of dehydroxylation occurs is dependent on the original structural state of the kaolin, the particle size, the density of packing, the pressure of water and a few other experimental conditions [10–13].

Metakaolin is used as supplement in cementitious material [14] and the calcinition conditions is one of the most important factors influencing the pozzolanic property (which is indicative of the lime-pozzolana reaction or how good and effective the pozzolan is) of the cementitious material produced [4, 15]. A pozzolan is defined as "a siliceous and aluminous material which, in itself, possesses little or no cementitious value but which will, in finely divided form in the presence of moisture, react chemically with calcium hydroxide at ordinary temperature to form compounds possessing cementitious properties" by the American Society for Testing and Materials (ASTM) [16].

The present paper aims to investigate the kinetics dehydroxylation of South African kaolin to metakaolin at temperature between 450 and 650 °C. Also Fourier Transformed infra-red spectroscopy was used to study the structural changes of metakaolin heated to different temperatures up to 950 °C within metakaolin state as well as the transformation to the spinel transition (950–1150 °C) and eventually the formation of mullite crystobillite (1200 °C). The changes in the spectra were studied as the function of fractional conversion of the ratios between AlO_6:AlO_4 and Si–O–Al:Si–O–Si. Also to measure the pozzolanic activity of the products that formed at the different thermal treatments, which will be used to determine the optimal calcination temperature for South African kaolin to be used as supplementary cementitious material.

Correspondence: Department of Chemistry, University of the Free State, Bloemfontein, 9300, Republic of South Africa.
E-mail: erasmuse@ufs.ac.za
Paper received: 20 July, 2015
Paper accepted: 10 November, 2015

EXPERIMENTAL

Chemicals and instruments

Kaolin (ALUSIL) was purchased from Serina Trading in South Africa. The chemical analysis as provided by the supplier is tabulated in Table 1. The kaolin used was in powder form and it has 72% minimum particles size less than 2 µm and maximum of 1% moisture content. All solid reagents (Merck, Sigma–Aldrich) were used without further purification and water was double distilled. Attenuated total reflectance Fourier Transformed infra-red (ATR FTIR) spectra were recorded on a Nicolet IS 50 infra-red spectrophotometer equipped with a diamond ATR. The TGA experiment was performed on a TGA/SDTA851^{e} coupled to a ThermoStar^{TM} Pfeifer vacuum mass spectrometer, at a heating rate of 10 °C.min^{-1} in air with the final temperature of 750 °C. X-ray photoelectron spectroscopy (XPS) data was recorded on a PHI 5000 Versaprobe system, with monochromatic AlKα X-ray source. Spectra were obtained using the aluminium anode (AlKα = 1486.6 eV), operating at 50 µm, 12.5 W and 15 kV energy. The survey scans were recorded at constant pass energy of 187.85 eV, and the detailed region scans at constant pass energy of 29.35 eV, with the analyzer resolution being ≤ 0.5 eV. The background pressure was 2×10^{-6} Pa. The XPS data was analysed, utilizing Multipak version 8.2c computer software [17] applying Gaussian–Lorentz fits (the Gaussian/Lorentz ratios were always > 95%).

Kinetic measurements of kaolin calcination/dehydroxylation

Kaolin was heated in a laboratory furnace at different temperatures (450, 475, 500, 550, 600 and 650 °C). Samples were taken at regular time intervals for ATR FTIR measurements. The kinetic rate constants under first order conditions were determined by monitoring formation and disappearance of the selected peaks.

Calculations. Pseudo first-order rate constants, k_{obs}, were calculated by fitting kinetic data to the first-order equation [18] $[A]_t = [A]_0 e^{-k_{obs}t}$ with $[A]_t$ and $[A]_0$ the absorbance of the indicated species at time t and at t = 0 [19].

Calcination/dehydroxylation of kaolin

Kaolin was heated in the laboratory furnace at different temperatures with 50 °C intervals (475, 500, 550, 600, 650, 750, 850, 950, 1050, 1150 and 1200 °C) till dehydroxylation was completed. After which ATR FTIR measurements were recorded for structure analysis.

Pozzolanic activity

The pozzolanic activity of the kaolin and metakaolin (kaolin calicined at various temperatures) were evaluated according to the Chapelle test [19]. A sample of either the kaolin or metakaolin (1 g) was mixed with 2 g $Ca(OH)_2$ in 250 cm^3 water. The suspension was subsequently boiled for 16 h. After which the suspension was cooled, a 250 cm^3 sucrose solution (60 g sugar in 250 cm^3 water) was added to the kaolin suspension and stirred for 15 min. The suspension was filtered and titrated with 0.1 M HCl, using phenolphthalein as indicator.

RESULTS AND DISCUSSION

ATR Fourier Transformed infra-red spectroscopy

The ATR FTIR of the South African kaolin studied is presented in Figure 1, the peak frequencies was allocated in accordance with previously published peak frequency assignments.[20,21] The four peaks observed between 3550 and 3750 cm^{-1}, which are characteristic of kaolinite, correspond to the hydroxyl stretching frequencies. The peak observed at 3620cm^{-1} is assigned to the inner O–H stretching frequency (Figure 1) which is bound to the octahedral Al. The other three peaks at 3686, 3669 and 3651 cm^{-1} is allocated to the stretching frequency of the surface O–H groups.

The main silica peaks are observed at 1002, 795 and 645 cm^{-1} which are the Si–O stretching, Si–O–Si stretching and bending frequencies respectively. Bands belonging to the alumina are found at 939 and 912 cm^{-1} representing respectively the Al–OH bending vibration and the –OH deformation linked to the $2Al^{3+}$.

Since there are no peaks observed between 1620-1642 cm^{-1}, which is the H–O–H bending of water, it can be assumed that there are very little to no free water within the sample. Bands observed at 1125, 1116, 752 and 685 cm^{-1} are attributed to the interference of clay minerals like quarts and muscovite.

The TGA plot of the thermal decomposition of the studied kaolin is shown in Figure 2. The percentage mass loss of the sample of kaolin by thermal dehydroxylation is 12.89%, with the onset and endset temperature being 443.12 and 534.04 °C, respectively.

Figure 3 shows the ATR FTIR of the thermal dehydroxylation and further transformation (structural changes) of kaolin at different temperatures. After calcination for prolonged periods of time at the desired temperature, it can clearly be seen that the hydroxyl peaks in the region 3550–3750 cm^{-1} disappeared, indi-

Table 1. The chemical analysis of the kaolin (ALUSIL)

Raw-oxide	SiO_2	Al_2O_3	Fe_2O_3	TiO_2	CaO	MgO	K_2O	N_2O	L.O.I.
Raw-content, mass%	45.20	37.20	0.35	0.90	0.016	0.08	0.20	0.13	13.50

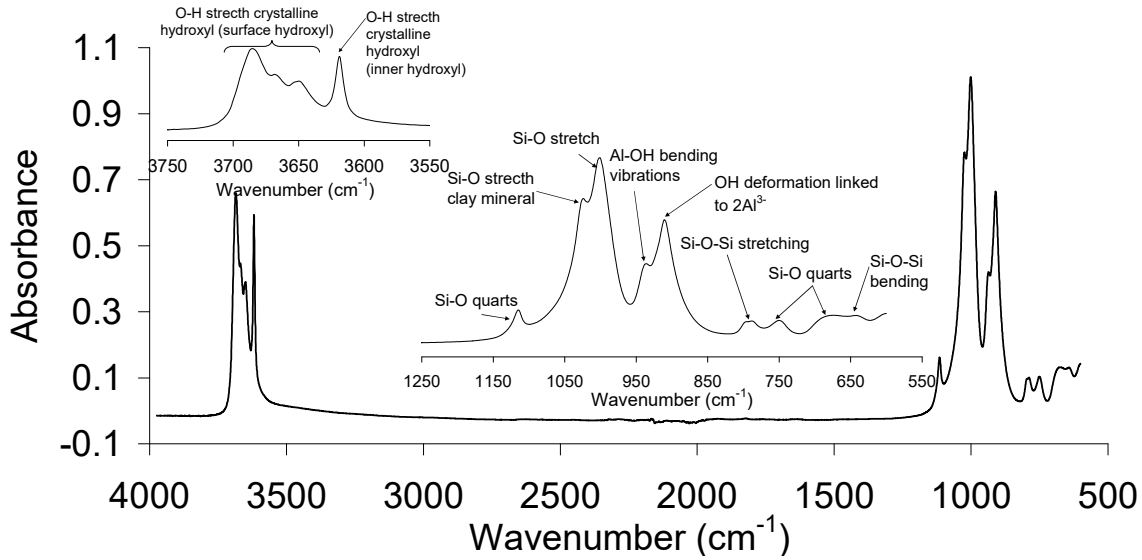

Figure 1. The infra-red spectra of the studied kaolin (Alusil), the insets show the peaks in more detail with their assignments.

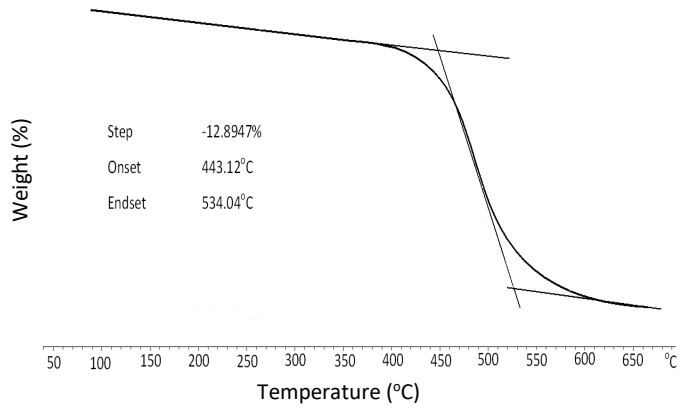

Figure 2. TGA plot of the thermal decomposition of kaolin (Alusil) heated at 10 °C/min.

cating the dehydroxylation of kaolin occurred. Below 450 °C, very little transformation of the silica and alumina occurred, and no dehydroxylation was observed. This result is further confirmed by the TGA data in Figure 2, which shows that below 450 °C very little to no dehydroxylation took place.

The spectra of the thermally treated kaolin shows very broad bands in the region of 600–1300 cm^{-1} with very little fine structure, there is an intense broad band at *ca*. 1100 cm^{-1} ($\nu_{Si–O–Al=}$) with a shoulder at 1200 cm^{-1} ($\nu_{\equiv Si–O–Si\equiv}$) and smaller bands at 800 ($\nu_{=Al–O–}$) and 667 cm^{-1} ($\nu_{=Al–O–}$). Further thermal treatment to produce mullite causes the peak at 1200 cm^{-1} ($\nu_{\equiv Si–O–Si\equiv}$) to increase in intensity as well as the appearance of two new bands at 890 ($\nu_{=Al–O–}$) and 740 cm^{-1} ($\nu_{=Al–O–}$).

The peaks focussed on in this study are listed in Table 2. The formation of the spinel phase and the formation of the mullite are connected to the appearance and disappearance of specific bands within the spectra.

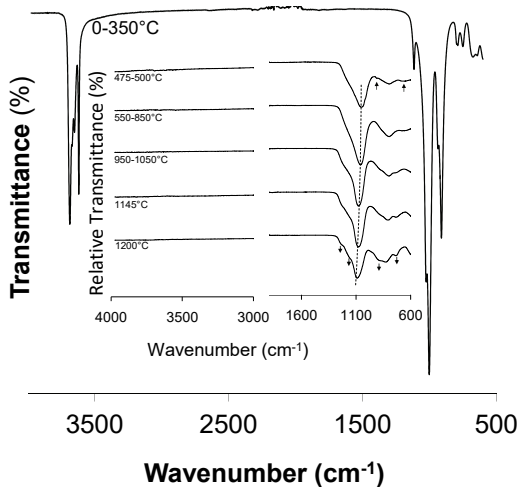

Figure 3. The FTIR ATR of the thermal dehydroxylation and further transformation of kaolin at different temperatures.

The disappearance of the =Al–O– stretching frequency of the octahedral AlO_6 and the antisymmetric stretching frequency of ≡Si–O–Al= at 667 and 1100 cm^{-1}

respectively as well as the appearance of the =Al–O– stretching frequency of the tetrahedral AlO_4 and the antisymmetric stretching frequency of ≡Si–O–Si≡ at 800 and 1200 cm^{-1} respectively were investigated.

Table 2. Fractional conversion of the ratio between AlO_6 (at 667 cm^{-1}) and AlO_4 (at 800 cm^{-1}) and the fractional conversion of the ratio between ≡Si–O–Al= (at 1100 cm^{-1}) and ≡Si–O–Si≡ (at 1200 cm^{-1}) at different temperatures during the thermal transformation of metakaolin to the spinel phase, as well as the fractional conversion of the ratio between AlO_6 and AlO_4 at different temperatures during the thermal transformation of the spinel phase to mullite

Temperature, °C	α of AlO_6:AlO_4	α of ≡Si-O-Al=:≡Si-O-Si≡
475	4.96	3.69
500	4.50	3.26
550	2.19	2.13
600	1.82	1.71
650	1.81	1.45
750	1.58	1.00
850	1.62	0.80
950	1.13	0.56
1050	1.08	0.55
1145	0.96	0.47
1200	0.03	0.01

The changes in the spectra were studied as the function of fractional conversion of the ratios between the AlO_6 and AlO_4 as well as ≡Si–O–Al= and ≡Si–O–Si≡, which is shown Figure 4 and defined by the equation below:

$$\alpha = \frac{i_0 - i_t}{i_0 - i_f}$$

where α is the fractional conversion, i_0 is the intensity of the band at time 0, i_t is the intensity of the band at time t and i_f is the intensity of the band at time final.

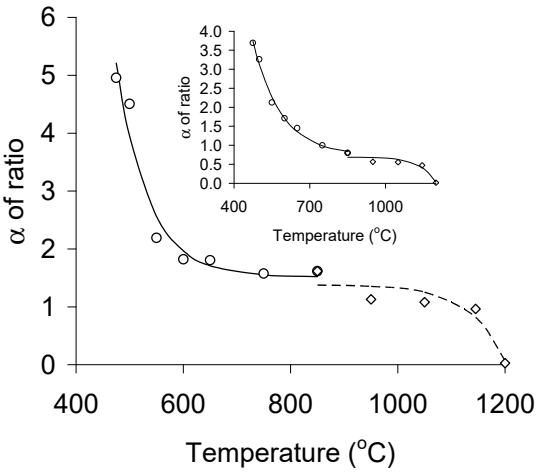

Figure 4. The fractional conversion of the ratio between AlO_6 and AlO_4. Inset: the fractional conversion of the ratio between ≡Si–O–Al= and ≡Si–O–Si≡ (1100 and 1200 cm^{-1}, respectively).

The fractional conversion of the ratio between ≡Si–O–Al= and ≡Si–O–Si≡ (1100 and 1200 cm^{-1} respectively) shows a sharp decrease between 475 and 850 °C, it then slightly flattens before going down even further when mullite is formed at 1200 °C. This indicates an increase in the formation of amorphous silica during the transformation to the spinel phase and eventually mullite formation. The fractional conversion decreases for the spinel formation and shows a k_{obs} value (observed rate constant) of 0.0089 s^{-1} for the fractional conversion of the ratio between ≡Si–O–Al= and ≡Si–O–Si≡ and a k_{obs} of 0.0168 s^{-1} for the fractional conversion of the ratio between AlO_6 and AlO_4. The influence on the rate of fractional conversion of the ratio between AlO_6 and AlO_4 is doubled that for the fractional conversion of the ratio between ≡Si–O–Al= and ≡Si–O–Si≡, showing that during the formation of the spinel phase the transformation of the Al is more pronounced than that for Si.

Further thermal treatment to produce mullite causes the peak at 1200 cm^{-1} to increase in intensity as well as the appearance of two new bands at 890 and 740 cm^{-1}, which is assigned to the symmetric stretching frequency of ≡Si-O-Al= and of ≡Si-O-Si≡ and the the =Al-O- stretching frequency of the tetrahedral AlO_4 in the mullite, as per reported values [22]. The mullite formation showed a k_{obs} value (observed rate constant) of 0.0165 s^{-1} for the fractional conversion of the ratio between ≡Si–O–Al= and ≡Si–O–Si≡ and a k_{obs} of 0.0156 s^{-1} for the fractional conversion of the ratio between AlO_6 and AlO_4. These two k_{obs} values are within experimental error the same and showed that during mullite formation, the transformation of the Al and Si were the same.

A kinetic study of the thermal dehydroxylation of kaolin to metakaolin was studied using ATR FTIR. The disappearance of the surface hydroxyl peaks at 3689 cm^{-1} and the inner hydroxyl peaks at 3620 cm^{-1} were followed (see Figure 5). Table 3 summarises the kinetic data, k_{obs} obtained at the different temperatures.

Numerous reports are available on the kinetics of dehydroxylation of kaolin, there is a debate between first order kinetics and diffusion controlled kinetics. Here we show that the hydroxyl groups on the surface of the kaolin are removed faster than the inner hydroxyls, at a temperature of 773 K, the k_{obs} value obtained for the disappearance of the surface hydroxyl peaks at 3689 cm^{-1} is 0.00128 s^{-1} as compared to the inner hydroxyl peaks at 3620 cm^{-1} is 0.00077 s^{-1}. This shows that even though both disappear with first order kinetics, the inner hydroxyl groups are dependent on diffusion control.

The pozzolanic activity of the thermally treated products (kaolin, metakaolin, spinel and mullite) that formed at the different thermal treatment of the kaolin

was measured using the Chapelle test, which measures amount of lime that can be bound by the metakaolin. It is measured in $Ca(OH)_2$/g and the higher the value the better the pozzolanic activity.

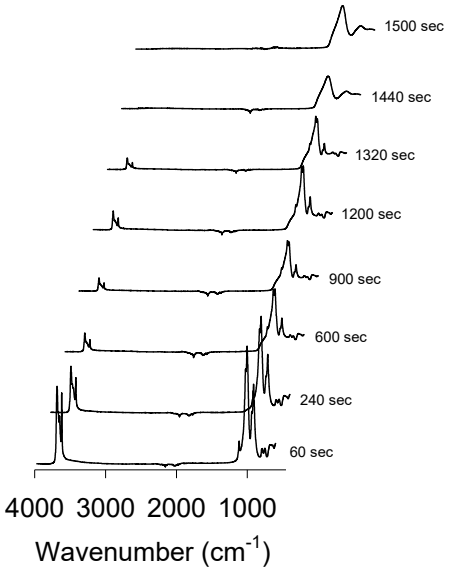

Figure 5. Stacked time scan of the calcination (dehydroxylation) of kaolin to metakaolin at 600°C.

Table 3. Data obtained for the calcination (dehydroxylation) of kaolin to metakaolin

Groups	Wavenumber, nm	T / K	k_{obs} / s^{-1}
Surface hydroxyls	3689	773	0.00128
		823	0.00159
		873	0.00263
		923	0.00364
Inner hydroxyls	3620	773	0.00077
		823	0.00106
		873	0.00220
		923	0.00291

The comparison of the consumed lime between the products formed at different thermal treatment temperatures are shown in Figure 6. A Bell type curve was formed, with the highest pozzolanic activity found at 650°C calcination temperature. The slope of the curve to the left (lower calcination temperatures) flattens to *ca*. 0.8 $Ca(OH)_2$/g at 0 °C. The slope of the curve to right (the higher calcination temperatures) slopes down to zero and eventually flattens to 0.073 $Ca(OH)_2$/g at 1200 °C (where mullite formed).

It was expected that kaolin heated below 400 °C would show the same low pozzolanic activity (0.8 $Ca(OH)_2$/g) as the kaolin that has not been subjected to thermal treatment. However, it has been reported that even though no major structural changes occur, there is a slight deformation in the octahedral sheets[23], which could possibly explain the pozzolanic values above 0.8 $Ca(OH)_2$/g.

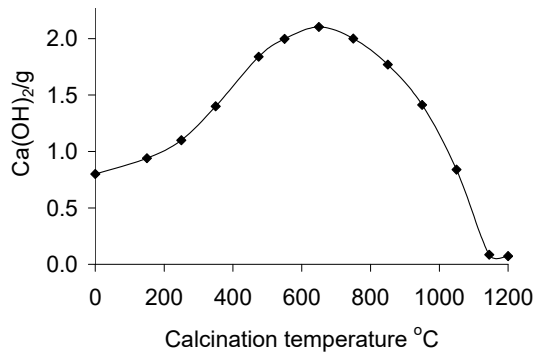

Figure 6. Pozzolanic activity of the calcined kaolin (measured in $Ca(OH)_2$/g) vs. calcination temperature.

Only the metakaolin formed at temperature between 350–950 °C had a pozzolanic activity above 1.3 $Ca(OH)_2$/g and only these 7 samples were considered to be pozzolanic. While the products formed at calcination temperature above 1050 °C has an even lower pozzolanic activity than the kaolin itself.

The temperature of the metakaolin prepared by calcination at 650 °C which has the highest pozzolanic activity (2.10 $Ca(OH)_2$/g), is slightly higher than other published data that also used this temperature. When metakaolin is used in the formation of geopolymers, the optimum calcination temperature is also reported to be between 500–700 °C [24] while a sharp decrease in strength of the geopolymer is reported above 1000 °C [25], all this corresponds to the pozzolanic activity reported in this publication in Figure 6. These results show that even when kaolin from different sources (different countries) are used, calcination at 650 °C results in the metakaolin with the best pozzolanic activity.

The results of the XPS studies of the kaolin, metakaolin (calined at 650 °C) and mullite (calcined at 1200 °C) are tabulated in Table 4.

Table 4. Results of the XPS studies of the kaolin (not calcined, as recieved), metakaolin (calined at 650 °C) and mullite (calcined at 1200 °C), showing the atomic % of Al, Si, C and O as well as the binding energies (eV) of the Al 2p and Si 2p peaks

Name : temperature of calcination, °C	at.% of Al	at.% of Si	Si:Al ratio	Binding energy, eV	
				Al $2p_{3/2}$	Si $2p_{3/2}$
Kaolin : 0	10.3	12.5	1.21	75.5	103.1
Metakaolin : 650	9.9	12.5	1.26	75.7	103.3
Mullite : 1200	7.7	11.7	1.52	74.0	102.5

All three of the samples (kaolin, metakaolin and mullite) showed that significant amounts of carbon were adsorbed their surface due to exposure to the atmosphere and this carbon's binding energy was set at 284.8 eV and was used for charge correction.

Firstly, it is important to note that Si:Al ratio obtained from the XPS data in the kaolin (not calcined sample) is 1.21, which is the same as the Si:Al ratio provided by the supplier information in Table 1, SiO_2:Al_2O_3 = 45.20%:37.20% = 1.22. After calcination at 650 °C the Si:Al ratio slightly increase to 1.26, but could be considered the same within experimental error. However, the sample calcined at 1200 °C (mullite) showed that the Si:Al ratio increase significantly to 1.52.

The binding energies for the Al 2p and Si 2p peaks were found to be at ca. 75.6 and 103.2 eV respectively for kaolin (not calcined sample) and metakaolin (calcined at 650 °C). These results are within experimental error the same, showing that electronic and chemical environment of the Al and Si did not change significantly after being calcined at 650 °C. However, calcination of kaolin at 1200 °C to produce mullite, caused the binding energy of both the Al 2p and Si 2p peaks to decrease by ca. 1.5 and 0.6 eV respectively (see Figure 7). The decrease in binding energy for the Al 2p peak is about three times more than that of the Si 2p peak, which is also accompanied by the decrease in Al content. It is well known that an increase in the Si:Al ratio is accompanied by a decrease in binding energies of both Si and Al.[26,27] This shows that there is a unique structural dissimilarity between the mullite and the metakaolin as well as the kaolin, caused by either a change in the electronic and/or the chemical environment.

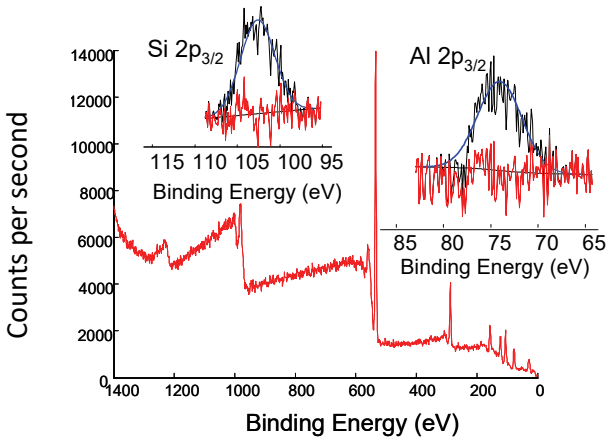

Figure 7. XPS spectra of the mullite, showing the detailed scans of the Si and Al regions.

CONCLUSION

The kinetics of dehydroxylation of South African kaolin at different temperatures (500–650 °C) was followed on FTIR ATR monitoring the disappearance of the four hydroxyl peaks between 3550 and 3750 cm^{-1}. The disappearance of the surface hydroxyl groups occurred at an observed rate constant of 0.00128 s^{-1} (at 500 °C) whereas the inner hydroxyl groups disappeared at an observed rate constant of 0.00077 s^{-1} (at 500 °C), which is one order of magnitude lower. This shows that even though both disappear with first order kinetics, it shows that the inner hydroxyl groups are dependent on diffusion control. The transformation of the kaolin to metakaolin, the spinel phase and mullite was investigated by means of FTIR ATR. The fractional conversion of the ratios between AlO_6:AlO_4 and Si–O–Al:Si–O–Si were calculated to be 0.0168 and 0.0089 s^{-1}, respectively, for the transformation to the spinel phase. The fractional conversion of the ratios between AlO_6:AlO_4 and Si–O–Al:Si–O–Si for the transformation to mullite were calculated to be 0.0165 and 0.0156 s^{-1}, respectively. The pozzolanic activities of the kaolin calcined at different temperature were tested using the Chappell test, showed that maximum pozzolanic activity is obtained when the kaolin is calcined at 650 °C. When the calcination temperature is above 1050 °C, the pozzolanic activity is even less than for uncalcined kaolin. The XPS of uncalcined kaolin, metakaolin (calcined at 650 °C) and mullite (calcined at 1200 °C) showed that the atomic ratio between Si and Al did not change from kaolin to metakaolin (Si:Al ≈ 1.2), but the mullite showed an atomic ratio of Si:Al = 1.52, implying that some deallumination occurred during calcination at high temperatures.

Acknowledgements

The authors acknowledge financial support from University of the Free State during the course of this study.

REFERENCES

[1] J. Konta, Clay and man: clay raw materials in the service of man, Appl Clay Sci. **10** (1995) 275–335.

[2] P. Ptacek, F. Soukal, T. Opravil, M. Noskova, J. Havlica, J. Brandstetr, Mid–infrared spectroscopic study of crystallization of cubic spinel phase from metakaolin, J. Sol. State Chem. **184** (2011) 2661–2667.

[3] M. Murat, M. Driouche, Chemical reactivity of thermally activated clay minerals estimation by dissolution in hydrofluoric acid, Cem. Concr. Res. **18** (1988) 221–228.

[4] B.R. Ilic, A.A. Mitrovic, L.R. Milicic, Thermal treatment of kaolin clay to obtain metakaolin, Hem. Ind. **64** (2010) 351–356.

[5] G. Kakali, T. Perraki, S. Tsivilis, E. Badogiannis, Thermal treatment of kaolin: the effect of mineralogy on the pozzolanic activity, Appl. Clay Sci. **20** (2001) 73–80.

[6] A. Shvarzman, K. Kovler, G.S. Grader, G.E. Shter, The effect of dehydroxylation/amorphization degree on poz-

zolanic activity of kaolinite,Cem. Concr. Res. **33** (2003) 405–416.

[7] J.A. Kostuch, G.V. Walters, T.R. Jones, High performance concrete incorporating metakaolin − a review, Concrete, **2** (1993) 1799–811.

[8] M. Arikan, K. Sobolev, T. Ertun, A. Yeginobali, P. Turker, Properties of blended cements with thermally activated kaolin, Constr. Build. Mater. **23** (2009) 62–70.

[9] J.J. Fripiat, F. Toussaint, Predehydroxylation State of Kaolinite, Nature **186** (1960) 627–628.

[10] L. Stoch, I. Waclawska, The kinetics of dehydroxylation of kaolinite, Polska Acad. Nauk. Prace Min. **1979** (1979) 59–79.

[11] M. Harman, I. Horvath, Relations between the morphology of particles in structurally and the kinetics of their dehydroxylation, Geol. Zbor. Geol. Carpath. **31** (1980) 115–124.

[12] F. Toussaint, J.J. Fripiat, M.C. Gastuche, Dehydroxylation of kaolinite, J. Phys. Chem. **67** (1963) 26–30.

[13] D. Yeskis, A.F. Koster van Groos, S. Guggenheim, The dehydroxylation of kaolinite, Amer. Miner. **70** (1985) 159–164.

[14] R. Talero, Comparative XRD analysis ettringite originating from pozzolan and from portland cement, Cem. Concr. Res. **35** (2005) 1269–1284.

[15] S. Chandrasekhar, Influence of metakaolinization temperature on the formation of zeolite 4a from kaolin, Clay Min. **31** (1996) 253–261.

[16] American Society for Testing and Materials (ASTM) C-125, Standard terminology relating to concrete and concrete aggregates; 2007.

[17] F. Moulder, W.F. Stickle, P.E. Sobol, K.D. Bomben, Handbook of X–ray Photo– 367 electron Spectroscopy, ULVAC–PHI, Inc., 370 Enzo, Chigasaki 253–8522, Japan, 368 1995, pp. 45, 57, 143.

[18] J.H. Espenson, Chemical Kinetics and Reaction Mechanisms, 2nd ed., McGraw–Hill, New York, 1995, pp. 15, 49, 70–75, 156.

[19] R. Largent, Estimation de l'activite pouzzolanique, Bull. Liaison Lab. Pont Chausees **93** (1978) 61–65.

[20] J.A. Gadsen, Infrared Spectra of Minerals and Related Inorganic compounds, Butterworths, London, 1975.

[21] B.J. Saikia, G. Parthasarathy, Fourier Transform Infrared Spectroscopic Characterization of Kaolinite from Assam and Meghalaya, J. Mod. Phys. **1** (2010) 206–210.

[22] P. Padmaja, G.M. Anilkumar, P. Mukundan, G. Aruldhas, K.G.K. Warrier, Characterisation of stoichiometric sol––gel mullite by fourier transform infrared spectroscopy, Int. J. Inorg. Mater. **3** (2003) 693–698.

[23] J. Komusinski, L. Stock, Dehydroxylation of kaolinite–group minerals: an ESR study, J. Thermal Anal. **29** (1984) 1033–1040.

[24] A. Elimbi, K.H. Tchakoute, D. Njopwouo, Effects of calcination temperature of kaolinite clays on the properties of geopolymer cements, Constr. Build. Mater. **25** (2011) 2805–2812.

[25] Z. Zhang, X. Yao, H. Zhu, Y. Chen, Role of water in the synthesis of calcined kaolin–based geopolymer, Appl. Clay Sci. **43** (2009) 218–223.

[26] S.L. Yong, D. Feng, G.C. Lukey, J.S.J van Deventer, Geopolymers: green chemistry and sustainable development solutions, Geopolymer Institut, Saint-Quintin, 2005, pp. 75–78.

[27] H. He, T.L. Barr, J. Klinowski, ESCA studies of framework silicates with the sodalite structure: (2) Ultramarine, J. Phys. Chem. **98** (1994) 8124–8127.

IZVOD

UTICAJ TOPLOTNE OBRADE NA SVOJSTVA KAOLINA

Elizabeth Erasmus

Department of Chemistry, University of the Free State, Bloemfontein, Republic of South Africa

(Naučni rad)

Kinetika dehidroksilacije kaolina iz Južne Afrike je pokazala da izdvajanje hidroksilnih grupa iz unutrašnjosti i sa površine, sledi kinetiku reakcije prvog reda, međutim brži nestanak hidroksilnih grupa sa površine u odnosu na nestanak iz unutrašnjosti ukazuje na značaj difuzione kontrole reakcije. Temperaturno zavisna transformacija kaolina, praćenjem odnosa AlO_6:AlO_4 i Si–O–Al:Si–O–Si, je pokazala da su k_{obs} vrednosti 0,0168 i 0,0089 s^{-1}, za transformaciju u spinel fazu, odnosno da su k_{obs} 0,0165 i 0,0156 s^{-1} za transformaciju u mulit fazu, redom. Kaolin kalcinisan na 650 °C pokazuje maksimalnu pucolansku aktivnost, a pucolanska aktivnost mulita je manja od aktivnosti nekalcinisanog kaolina. XPS ukazuje na to da se atomski odnos Si i Al ne menja pri prelasku kaolina u metakaolin (Si:Al ≈ 1,2), međutim kod mulita je utvrđen odnos Si:Al = 1,52.

Ključne reči: Dehidroksilacija • Kaolin • Metakaolin • Infracrveno • Pucolanska aktivnost • Mulit